Title: Relationship between floristic similarity and vegetated land surface phenology: Implications for the synoptic monitoring of species diversity at broad geographic regions

Authors: Andrés Viña[1], Mao-Ning Tuanmu[1], Weihua Xu[2], Yu Li[1], Jiaguo Qi[3], Zhiyun Ouyang[2] and Jianguo Liu[1]

Affiliations:

[1] *Center for Systems Integration and Sustainability, Department of Fisheries and Wildlife, Michigan State University, East Lansing, MI, USA*

[2] *State Key Lab of Urban and Regional Ecology, Research Center for Eco-Environmental Sciences, Chinese Academy of Sciences, Beijing, China*

[3] *Center for Global Change and Earth Observations, Department of Geography, Michigan State University, East Lansing, MI, USA*

Corresponding Author: Andrés Viña
Center for Systems Integration and Sustainability
1405 S. Harrison Road
Suite 115 Manly Miles Bldg.
Michigan State University
East Lansing, MI 48823-5243
U. S. A.
Phone: (517) 432-5078
e-mail: vina@msu.edu

Published in Remote Sensing of Environment 121 (2012), pages: 488–496

Abstract

Assessing species composition and its changes through time across broad geographic regions are time consuming and difficult endeavors. The synoptic view provided by imaging remote sensors offers an alternative. But while many studies have developed procedures for assessing biodiversity using multi- and hyper-spectral imagery, they may only provide snapshots at particular months/seasons due to the seasonal variability of spectral characteristics induced by vegetated land surface phenologies. Thus, procedures for remotely assessing biodiversity patterns may not fully represent the biodiversity on the ground if vegetated land surface phenologies are not considered. Using Mantel tests, ordinarily least square regression models and spatial autoregressive models, we assessed the relationship between floristic diversity and vegetated land surface phenologies, as captured by time series of vegetation indices derived from data acquired by the Moderate Resolution Imaging Spectroradiometer (MODIS). The relationship was calibrated with data from temperate montane forests of the Qinling Mountains region, Shaanxi Province, China. Our results show that floristically similar areas also exhibit a comparable similarity in phenological characteristics. However, phenological similarity obtained using the Visible Atmospherically Resistant Index (VARI), a spectral vegetation index found to be not only sensitive to changes in chlorophyll content but also linearly related with the relative content of foliar anthocyanins, exhibited the strongest relationship with floristic similarity. Therefore, analysis of the temporal dynamics of pigments through the use of satellite-derived metrics, such as VARI, may be used for evaluating the spatial patterns and temporal dynamics of species composition across broad geographic regions.

1. Introduction

Information on the spatial patterns of biodiversity across broad geographic regions and their changes through time is important for many applications in ecology, biogeography and conservation biology, among many others (Ferrier 2002; Liu and Ashton 1999). However, acquisition of such information requires a synoptic and large spatial extent view that is seldom provided by the limited spatial extents of traditional and labor-intensive field surveys. The direct use of synoptic data acquired by remote sensors constitutes an alternative approach for analyzing the spatial patterns of biodiversity from local to regional and continental scales (Turner et al. 2003).

Many attempts to assess biodiversity patterns through remote sensing techniques have relied on the relationships between biodiversity and land cover types (Laurent et al. 2005), the latter obtained from numerical classifications of remotely sensed data (Nagendra 2001). But information acquired through such relationships is insufficient for assessing biodiversity patterns within a single land cover type, which by definition is assumed to be spatially homogeneous. Alternatively, recent studies have discerned pixel-based relationships between patterns of biodiversity across broad geographic regions and multispectral imagery (Rocchini 2007; Rocchini et al. 2010; Thessler et al. 2005; Tuomisto et al. 2003a). Others have amassed spectral libraries of several plant species to develop relationships based on hyper-spectral imagery (Asner and Martin 2008, 2009; Carlson et al. 2007). Although successful, many of these methods are constrained to particular geographic locations, individual species and/or species assemblages and have not been widely adopted due to the low availability and high cost of the required remotely sensed data, particularly those acquired by hyper-spectral imaging sensors.

Further, and perhaps more important, these methods do not necessarily account for the spectral variability that occurs in response to vegetation phenology.

In contrast, multispectral synoptic data acquired by different operational satellite sensor systems, such as the Advanced Very High Resolution Radiometer (AVHRR) or the Moderate Resolution Imaging Spectroradiometer (MODIS) on-board the National Aeronautics and Space Administration's (NASA) Terra and Aqua satellites, are freely available and provide nearly global coverage. While these data are being acquired in broad spectral bands and at coarse spatial resolutions (ca. 250x250 m/pixel or larger), their usefulness stems from their high temporal resolution (e.g., daily acquisition). This makes them suitable for assessing land surface phenology and its changes through time in response to natural (de Beurs and Henebry 2008a; Viña and Henebry 2005) and human processes (de Beurs and Henebry 2004, 2008b). From the perspective of biodiversity assessment, land surface phenology (as detected by remote sensors collecting data at a high frequency; e.g., MODIS) has been used to map the distribution of plant functional types (Sun et al. 2008), to evaluate the spatial distribution of understory species (Tuanmu et al. 2010), to assess the probability of occurrence of invasive species (Morisette et al. 2006), to analyze wildlife habitat suitability (Tuanmu et al. 2011; Viña et al. 2008; Viña et al. 2010), and to evaluate species richness (Fairbanks and McGwire 2004) and species turnover across space (He et al. 2009). However, in all these cases vegetation phenology has been characterized using remotely sensed metrics such as the normalized difference vegetation index (NDVI), the enhanced vegetation index (EVI) or the wide dynamic range vegetation index (WDRVI), which are related more to the variability of

photosynthetic biomass, thus chlorophyll content, and less to the variability in the content of other pigments.

Foliar pigment content and composition have been shown to be related to species diversity (Asner and Martin 2008, 2009; Carlson et al. 2007), but we hypothesize that because plant species assemblages have distinctive phenologies associated with changes in pigment content and composition, a close relationship may exist between floristic similarity and the similarity in the seasonality of pigment expression. Thus, the seasonality of pigment expression may constitute a suitable surrogate for evaluating the spatio-temporal dynamics of floristic diversity patterns across broad geographic regions. Here we show the results of a study performed to evaluate this proposition.

2. Methods

2.1. Study region

The Qinling Mountains lie in an east-west direction in the southern portion of Shaanxi Province, China (Fig. 1). Because it forms the divide between two major watersheds drained by the Yellow and Yangtze rivers, this mountain region forms a natural boundary between northern and southern China and also constitutes a climatic transition, from cold and dry in its northern slopes to warm and wet in its southern slopes. Due to this north-south climatic transition and its gradients in elevation (Fig. 1), the Qinling Mountains harbor high biodiversity, supporting more than 3,000 plant species, over 300 bird species, and more than 85 mammal species, including the endangered giant panda (Pan et al. 1988). The distribution of vegetation in the Qinling Mountains follows an elevation gradient, with coniferous forests located mostly above 2500m, mixed

broadleaf/coniferous forests located mostly between 2000 and 2500m and broadleaf deciduous forests located mostly between 1400 and 2000m (Yue et al. 1999). Areas below 1400m are dominated by agricultural activities, which historically remained below 1400m since climatic and edaphic conditions above this elevation restrict year-round cultivation (Loucks et al. 2003). But human disturbance above 1400m has increased during recent decades, particularly in the form of logging, expansion of human settlements, and infrastructure development (e.g., roads), which have fragmented and degraded the forests of the region (Loucks et al. 2003). In response, 15 nature reserves have been established primarily for the conservation of giant pandas and their habitat (Fig. 1). These reserves also promote the conservation of other taxa, since the giant panda habitat comprises different types of forest ecosystems (Reid and Hu 1991).

2.2. Field Data

Between June and August of 2007 and 2008 a total of 104 circular plots (10 m radius) were randomly established in broadleaf deciduous, coniferous and mixed forests across the study region, within an elevation range of 1000 to 3000 m (Fig. 1). Plots were located at least 1 km inside the forests to minimize edge effects. Species composition of all tree stems (with a diameter at breast height, dbh ≥ 5 cm) within each plot was recorded, together with forest structural characteristics (i.e., stem density, basal area and canopy closure) and topographic variables (i.e., elevation, slope and aspect). The center of each plot was geo-referenced using Global Positioning System (GPS) receivers, which were also used to collect elevation data. Stem density was established by counting all the stems (dbh ≥ 5 cm) within each plot. Basal area was determined from the measured dbh

of all the trees counted in the plot. Per-plot canopy closure was determined as the average canopy closure estimated in three to five images of the canopy taken with a digital camera at breast height facing upward. Slope and aspect (i.e., slope azimuth) were determined using a clinometer and a compass. The aspect was later converted into soil moisture classes, ranging from 1 (dry) to 20 (wet). These discrete soil moisture classes derive from the observation that north-facing slopes in mountainous regions of the temperate zone in the northern hemisphere tend to be more moist than south-facing slopes, as they tend to receive less direct solar radiation (Parker 1982). As understory bamboo is a conspicuous and dominant characteristic of the forests in the Qinling Mountains, we also recorded bamboo species composition in each plot, when present.

2.3. Remotely Sensed Data

A time-series of 184 images acquired between January 2004 and December 2007 by the MODIS system onboard NASA's Terra satellite (MOD09A1 – Collection 5) was used to analyze land surface phenology in the pixels containing the field plots. This image dataset is made up of eight-day composite surface reflectance values collected in seven spectral bands, and corrected for the effects of atmospheric gases, aerosols and thin cirrus clouds (Vermote et al. 1997). Land surface phenology was assessed through the temporal analysis of four different vegetation indices calculated from the MODIS surface reflectance time series: the Normalized Difference Vegetation Index (NDVI) (Rouse et al. 1973), the Wide Dynamic Range Vegetation Index (WDRVI) (Gitelson 2004), the Enhanced Vegetation Index (EVI) (Huete et al. 1997) and the Visible Atmospherically Resistant Index (VARI) (Gitelson et al. 2002) (Table 1).

The NDVI has been widely used for the analysis of land surface phenology (de Beurs and Henebry 2004) and its temporal variability has been associated with biodiversity patterns (He et al. 2009). However, because NDVI approaches an asymptotic saturation under conditions of moderate to high biomass, other vegetation indices, such as the EVI and the WDRVI, were developed and their use has increased over the last few years. The EVI is a feedback-based soil and atmospherically resistant index specifically designed for the MODIS system that has been successfully used to evaluate phenological patterns in high biomass systems such as tropical humid forests (Xiao et al. 2006). The WDRVI is a non-linear transformation of the NDVI that has been shown to exhibit a linear relationship with the fraction of photosynthetically active radiation absorbed by vegetation (Viña and Gitelson 2005). Phenological asynchronies detected using this index have been successfully used to discriminate individual understory bamboo species (Tuanmu et al. 2010) and to assess wildlife habitat suitability at local (Viña et al. 2008) and regional (Viña et al. 2010) scales. Because these three indices are based on the contrast between the near-infrared and red spectral regions (Table 1), they mainly provide information on spatio-temporal changes in the amount of photosynthetic biomass. Thus, they are responsive to changes in chlorophyll content but may neglect phenological dynamics associated with other pigments and processes. In response, alternative vegetation indices based on different spectral bands have been developed. Such is the case of the VARI (Table 1), which has been shown to be sensitive not only to changes in chlorophyll content (Gitelson et al. 2002; Perry and Roberts 2008), but also to changes in the relative content of other foliar pigments, particularly anthocyanins (Viña and Gitelson 2011). Therefore, the VARI is useful for detecting

changes associated with phenophases that go beyond the seasonal variability of photosynthetic biomass (e.g., flowering, fruiting, senescence) (Viña et al. 2004). This index has also been used to detect live fuel moisture (Roberts et al. 2006), canopy moisture content (Stow et al. 2005) and water stress (Perry and Roberts 2008), using various remote sensors.

To reduce the effects of a temporally and spatially extensive cloud cover observed over the study region, we smoothed the time series of each vegetation index by means of an adaptive filter (Savitzky and Golay 1964). In addition, to reduce the inter-annual variability caused by short-term climate fluctuations, we obtained a final time series of 46 eight-day composites for each vegetation index (Table 1), using the maximum value composite approach (Holben 1986) applied across years (i.e., 2004-2007).

2.4. Numerical Analyses

To evaluate floristic similarity among field plots, inter-plot similarity index matrices were calculated using both presence-absence data, as well as abundance (i.e., stem density) data. In the case of presence-absence we used the Jaccard index (Jaccard 1908), and in the case of abundance we used the Morisita index (Morisita 1959). The Jaccard index was calculated for the tree species, as well as for the tree and bamboo species combined, while the Morisita index was calculated for the tree species only, since stem densities of tree and bamboo species are not comparable. To evaluate the phenological similarity among the pixels where the field plots were located, we calculated inter-pixel Euclidean distance matrices (converted to similarity by changing their signs) for each of the four vegetation index image time series (i.e., NDVI, EVI,

WDRVI and VARI). The correlation between floristic and phenological similarity matrices was calculated using Mantel tests, to adjust for the increased number of cases deriving from the use of distances (Legendre 2000). The significance of the Mantel tests was determined through a Monte Carlo permutation analysis in which the rows and columns in one of the similarity matrices were randomly permuted 999 times. The significance measure corresponds to the number of times the Mantel correlation coefficient of the permuted matrices exceeded the original (i.e., non-permuted) coefficient (Legendre 2000). To control for the potential effects of geographic distance (e.g., spatial autocorrelation) (Borcard et al. 1992), partial Mantel tests (Legendre 2000) were also calculated using an inter-plot geographic distance matrix as a co-variable.

Linear models were developed to predict floristic similarity based on phenological similarity. For this, ordination procedures were used to locate the field plots in multi-dimensional coordinate systems based on their floristic and phenological similarities. For floristic similarity, a non-metric multidimensional scaling (NMDS) procedure was employed, which maximizes the rank-order correlation between the similarity measures and the relative distances within the ordination space (Legendre and Legendre 1998). For phenological similarity, a principal components analysis (PCA) was applied to the vegetation index image time series. Multiple linear regression models were then developed using the floristic ordination axes (i.e., derived from the NMDS) as dependent variables, and the phenological ordination axes (i.e., derived from the PCA) as independent predictive variables. Model residuals were used to evaluate spatial autocorrelation through the calculation of Moran's I correlograms (Legendre and Legendre 1998). If spatial autocorrelation of the residuals was significant, spatial

autoregressive models (Besag 1974; Lichstein et al. 2002) were developed to estimate spatially unbiased regression coefficients. Lag, error and mixed autoregressive models were computed (Lichstein et al. 2002) and the most appropriate for our datasets was selected.

To invert and validate the models, the entire field dataset (i.e., 104 field plots) was divided into *k* mutually exclusive groups following a *k*-fold cross-validation partitioning design (Kohavi 1995). In our case the data were randomly split into $k = 3$ sets, two of which were used iteratively for model calibration (ca. 70 field plots) and the remaining (ca. 34 field plots) for validation. The advantages of this cross-validation method are that: (1) it reduces the dependence on a single random partition into calibration and validation data sets; and (2) all observations are used for both calibration and validation, with each observation used for validation exactly one time. Predictions of the floristic ordination axes (i.e., NMDS axes) values for every field plot were obtained using their corresponding phenological ordination axes values (i.e., from the PCA) and the coefficients of the linear regressions described above. An Euclidean distance matrix among all field plots was then calculated based on the predicted NMDS axes values. This matrix was correlated (using a Mantel test with 999 random permutations) with the inter-plot floristic similarity matrix obtained using the Jaccard index for the tree and bamboo species combined, described above. Through this cross-validation procedure we inverted the model to assess the operational accuracy of the prediction of floristic similarity using phenological similarity.

3. Results

3.1. Spatio-temporal characteristics of land surface phenology

The average temporal variability of the forests studied exhibited the typical seasonal pattern of the temperate region (i.e., high and low vegetation index values during seasons with high and low sun angles, respectively). This pattern was depicted by the four different vegetation indices evaluated (Fig. 2A). However, the indices exhibited different temporal dynamics in the inter-pixel variance among the MODIS pixels where the field plots were located (Fig. 1). For instance, the NDVI exhibited the highest inter-pixel variance during winter and the lowest during summer, while the EVI exhibited an opposite pattern, with the highest variance during summer and the lowest during winter (Fig. 2B). The WDRVI exhibited the highest inter-pixel variance during winter and spring, while the VARI exhibited the highest variance during spring and summer (Fig. 2B). These distinctive patterns in the timing of highest and lowest inter-pixel variance show the particular sensitivities of each vegetation index to differences among the forests of the study region throughout the year.

The NDVI, the EVI and the WDRVI exhibited a significant negative correlation with elevation during late spring and summer (Fig. 2C). In contrast, the VARI experienced a significant negative correlation during spring and autumn (Fig. 2C). Therefore, while the NDVI, the EVI and the WDRVI exhibited unimodal temporal patterns in their relationship with elevation, the VARI exhibited a bi-modal pattern (Fig. 2C).

3.2. Floristic and structural characteristics

As shown by the relationship between phenological patterns and elevation (Fig. 2C), the vegetation of the study region is highly influenced by elevation. However, with the exception of canopy closure (Fig. 3A), no statistically significant differences were found in average forest structural characteristics evaluated along this gradient (Figs. 3B-D). Nevertheless, while at elevations between 1000 and 2500m the species richness did not exhibit a significant trend with elevation, above 2500m the number of species per plot exhibited a significant decline (Fig. 3D). Thus, a threshold of significant reduction in species richness was conspicuous at elevations of ca. 2500 m.

With respect to species composition, a total of 115 tree species were sampled in the 104 field plots surveyed (see on-line Supplementary Data). The species *Quercus aliena*, *Betula albo-sinensis*, *Prunus scopulorum*, *Toxicodendron vernicifluum*, and *Pinus armandii* were the most widespread (i.e., each occurring in more than 20% of the plots). Understory bamboo was a particularly conspicuous feature of the forests in the study region, as it was found in ca. 82% of the field plots. However, most of the bamboo sampled belonged to three species: *Fargesia qinlingensis* (present in ca. 38% of the plots), *Bashania fargesii* (present in ca. 37% of the plots) and *F. dracocephala* (present in ca. 11% of the plots). These three species were among the most widely distributed in the study region.

3.3. Relationship between floristic and phenological similarities

A strong and significant relationship was found between the similarity in floristic composition and the similarity in phenology. All Mantel tests performed to assess this

relationship showed significant ($p < 0.001$) correlations (Table 2). However, Mantel correlations were highest using the phenological similarity matrix based on the VARI (Table 2). In addition, Mantel correlations were higher when using information on tree and bamboo species combined, than when only using information on tree species (Table 2). In the case of tree species information alone (i.e., excluding bamboo), Mantel correlations were higher when using presence-absence data (i.e., using the Jaccard index), than when using abundance data (i.e., using the Morisita index; Table 2). Partial Mantel tests, using geographic distance as a co-variable to account for potential spatial autocorrelation among field plots, exhibited higher Mantel correlations in all cases, with the exception of those using the phenological similarity matrix based on the NDVI image time series (Table 2).

3.4. Prediction of floristic similarity using phenological similarity

A Non-Metric Multidimensional Scaling (NMDS) ordination procedure was applied to the inter-plot floristic similarity matrix obtained using presence-absence data of tree and bamboo species combined (i.e., using the Jaccard index), since this matrix exhibited the highest Mantel correlation coefficients with phenological similarity matrices (Table 2). The NMDS procedure generated two orthogonal axes that represent a two-dimensional floristic space. Patterns in the distribution of topographic characteristics (i.e., elevation, slope and aspect) among field plots, together with forest types (i.e., predominantly coniferous, predominantly deciduous broadleaf or mixed coniferous-deciduous) are conspicuous in this floristic space (Fig. 4). For instance, the elevational gradient follows a right-left pattern (Fig. 4A), while aspect, expressed as discrete relative

soil moisture classes (Parker 1982), follows an upper-right lower-left pattern in the floristic space (Fig. 4B). Although not as clear, slope tends to show a lower-left, upper-right pattern (Fig. 4C). Finally, while mixed forests exhibited no clear pattern, predominantly coniferous forests tended to be located towards the upper-left, and predominantly deciduous broadleaf forests tended to be located toward the lower part of the floristic space (Fig. 4D). However, elevation exhibited the highest effect since the first NMDS axis exhibited a statistically significant ($p < 0.05$) negative linear relation with elevation (Fig. 5A).

A principal components analysis was applied on the image time series of the VARI, as the similarity matrix of this index exhibited the highest Mantel correlation coefficients with the floristic similarity matrices (Table 2). We retained the first six principal components, which together explained ca. 99% of the image time series variance. Similar to the NMDS, the first principal component exhibited a statistically significant ($p < 0.05$) negative linear relationship with elevation (Fig. 5B). In addition, principal component loadings show different sensitivities of the VARI index along the year. For instance, the first principal component exhibited high positive loadings along the year, but particularly during spring and autumn (Fig. 6). Thus, loadings of this component exhibited a similar bi-modal temporal pattern (albeit with a different sign) as the bi-modal temporal pattern observed with elevation (Fig. 2C). This is related to the fact that the first principal component of the VARI time series was significantly and negatively related to elevation (Fig. 5B). The second component exhibited the highest positive and negative loadings during summer and winter, respectively, while the third component was positively related with autumn VARI values but negatively related with

spring values (Fig. 6). This reflects the sensitivity of VARI to changes in the forests of the region during these seasons.

Significant linear models to predict floristic similarity (i.e., NMDS axes) using phenological similarity (i.e., principal component axes) were obtained (Table 3). Thus, phenological ordination axes obtained using satellite imagery with a high temporal resolution may be used as significant predictors of floristic ordination axes obtained using data from field surveys. The regression model developed for the first floristic NMDS axis was not affected by spatial autocorrelation. In contrast, the model developed for the second floristic NMDS axis did exhibit significant spatial autocorrelation (Table 3). Therefore, we developed an ordinary least square regression model in the first case, and a spatial autoregressive model in the second case. As the lag coefficient in the spatial autoregressive model was significant ($p < 0.001$; Table 3) while the spatial correlation coefficient in the error model was not, the spatial lag model was selected as the most appropriate spatial autoregressive model for our data. In these linear models, the first, third, fourth and sixth principal components were significant predictors of the first NMDS axis, while the second and fourth components constituted significant predictors of the second NMDS axis (Table 3).

Results of the model inversion using the *k*-fold cross-validation partitioning design (k=3) showed a statistically significant ($p<0.001$) Mantel correlation of 0.37. This Mantel correlation was calculated using the Euclidean distance matrix derived from the predicted NMDS axes (using PCA in VARI time series) and the observed Jaccard Index matrix derived from presence/absence of tree and bamboo species observed in the field.

Therefore, inter-pixel phenological similarity obtained using the VARI image time series can be reasonably used for assessing floristic similarity.

4. Discussion

The results of this study show that there is a significant relationship between floristic similarity and phenological similarity obtained using all four vegetation indices evaluated. These results agree with a previous study showing a significant relationship between MODIS-NDVI time series and species composition (He et al. 2009). However, in this study it was the phenological similarity based on the VARI that exhibited the highest correlation. Several studies have shown that VARI is sensitive to changes in the photosynthetic biomass (thus chlorophyll content) not only at foliar (Viña and Gitelson 2011) but also at canopy levels using both close range (Gitelson et al. 2002) and remote (Almeida de Souza et al. 2009; Perry and Roberts 2008) sensors. But because anthocyanins absorb radiation primarily in the green spectral range (i.e., around 540–560 nm), it has been reported that vegetation indices using the green spectral region (such as VARI) are sensitive to their presence (Gitelson et al. 2006a; Gitelson et al. 2001). Furthermore, it has been reported that VARI is a suitable surrogate of the relative composition of foliar anthocyanins in at least five tree species (Viña and Gitelson 2011). Therefore, while changes in other canopy components may also be important, changes in pigment content and composition are important drivers of the seasonal variability of VARI.

Previous studies have found that information on the amount and composition of foliar pigments can be used to assess floristic diversity (Asner and Martin 2008, 2009;

Carlson et al. 2007). The results of this study suggest that information on the seasonal variability of pigment content and composition, using metrics such as VARI, may improve this assessment. In addition, as VARI can be easily obtained using currently operational satellites, it allows evaluating floristic diversity patterns across broad geographic regions. Nevertheless, a fundamental assumption in these analyses was that the sampled forest stands are homogeneous, at least within each of the MODIS pixels evaluated. Thus, the species composition in each field plot was assumed to be representative of the entire MODIS pixel. The strong and significant relationship found between floristic and phenological similarities suggests that this assumption was satisfactory. However, floristic similarity based on presence-absence data (i.e., using the Jaccard similarity index) exhibited a stronger correlation with phenological similarity than the similarity obtained based on abundance (i.e., stem density) data (i.e., using the Morisita similarity index). These results seem to relate to the scale mismatch between field plots and MODIS pixels, since the species present in a field plot may be representative of the entire MODIS pixel, but relative species abundance per plot may not fully represent that of the entire pixel. In addition, higher correlations between floristic and phenological similarities were obtained using both tree and bamboo species composition, than when using tree species alone. Thus, bamboo species, which are conspicuously dominant understory components in the forests of the region, strongly contribute to the overall spectral and phenological characteristics of the forest canopy (Tuanmu et al. 2010; Viña et al. 2008). The use of phenological similarity to evaluate spatial patterns of floristic diversity, therefore, provides information on both overstory and understory canopy components. This may also explain why vegetation phenology

can be successfully used for identifying the occurrence of understory bamboo species growing below the canopy of trees (Tuanmu et al. 2010).

Environmental characteristics influence not only the patterns of floristic diversity and vegetation phenology but also their relationship. For instance, the geographic distance among plots had a significant effect on the relationship between floristic and phenological similarities (e.g., partial Mantel correlations tended to be higher when using a matrix of inter-plot geographic distances as a co-variable). This result suggests that species dispersal (which is a function of geographic distance) may constitute an important characteristic structuring the spatial patterns of tree species in the study region, as has been found in other forest ecosystems (Tuomisto et al. 2003b). Therefore, spatial autocorrelation should be considered in models based on vegetation phenology for predicting floristic diversity patterns. Topographic characteristics such as slope and aspect also influence floristic diversity patterns, but elevation was the most important environmental characteristic evaluated that directly contributed to structuring not only the species composition [as shown for several other taxa and under different geographic settings (Hofer et al. 2008; Rahbek 1995)], but also vegetation phenology. For example, the NDVI, the EVI and the WDRVI showed significant negative relationships with elevation, but mainly during spring and summer. Since these vegetation indices have been found to be significantly related with gross primary productivity (Gitelson et al. 2008; Gitelson et al. 2006b; Jahan and Gan 2009; Vourlitis et al. 2011; Xiao et al. 2004; Xiao et al. 2005), this temporal pattern in their relationship with elevation suggests that primary productivity of the forests of the study region during the growing season may decrease with elevation. In contrast, the VARI was particularly interesting since it

showed the highest negative correlation coefficients during spring and autumn, thus exhibiting a bi-modal temporal pattern in its relationship with elevation. This may be explained by the fact that foliar anthocyanins [whose relative contents were found to be linearly related with VARI (Viña and Gitelson 2011)] are produced not only during autumn senescence, but also in young emerging leaves (Lee et al. 1987). In the study region the leaves of trees start to emerge around early May (ca. day of the year 121-129) (Pan et al. 1988). In fact, this time corresponded with the period of maximum VARI variance among the pixels where the field plots were located (see Fig. 2C). Thus, the strong relationship between VARI and elevation during spring and autumn suggests that the timing of phenophases such as leaf emergence and senescence may be driven by the differences in species composition along the elevation gradient (Nautiyal et al. 2001; Negi et al. 1992; Ziello et al. 2009).

5. Conclusions

We have presented here a novel approach for synoptically assessing the spatio-temporal patterns of floristic diversity across broad geographic regions, and successfully applied it in temperate montane forests of China. If the hypothesis underlying this approach (i.e., a strong relationship between floristic and phenological similarities) is applicable in regions exhibiting less pronounced seasonal dynamics, it may also prove to be a valuable tool for mapping and monitoring floristic diversity patterns in other ecosystems around the globe. This has many practical implications, including its use in studies analyzing spatial congruence among communities or guilds (McKnight et al. 2007) or monitoring biodiversity dynamics under a changing environment (e.g., land use/cover

change, climate change). The approach may also aid in the development of management actions oriented towards a more inclusive conservation of biodiversity across broad geographic regions (Ferrier 2002; Xu et al. 2006). For example, knowledge of the spatial patterns of biodiversity can be used to analyze the proportion of the regional biodiversity protected inside nature reserves (Scott et al. 2001), and thus target further conservation actions.

Acknowledgments

The study was supported by the National Aeronautics and Space Administration (NASA), the U. S. National Science Foundation (NSF) and the National Natural Science Foundation of China. We thank Gaodi Dang for his invaluable assistance in identifying tree and bamboo species composition in our field plots, as well as William J. McConnell, Duccio Rocchini and two anonymous reviewers for providing helpful comments and suggestions to improve the manuscript's clarity. The Land Processes Distributed Active Archive Center (LP DAAC), located at the U.S. Geological Survey (USGS) Earth Resources Observation and Science (EROS) Center (lpdaac.usgs.gov) is also acknowledged for the MODIS data used in the study,

References

Almeida de Souza, A., Soares Galvão, L., & dos Santos, J.R. (2009). Índices de vegetação derivados do sensor Hyperion/EO-1 para estimativa de parâmetros biofísicos de fitofisionomias de cerrado. In, *XIV Simposio Brasileiro de Sensoramiento Remoto* (pp. 3095-3102). Natal, Brasil: INPE

Asner, G.P., & Martin, R.E. (2008). Spectral and chemical analysis of tropical forests: Scaling from leaf to canopy levels. *Remote Sensing of Environment, 112*, 3958-3970

Asner, G.P., & Martin, R.E. (2009). Airborne spectranomics: Mapping canopy chemical and taxonomic diversity in tropical forests. *Frontiers in Ecology and the Environment, 7*, 269-276

Besag, J. (1974). Spatial interaction and the statistical analysis of lattice systems. *Journal of the Royal Statistical Society B*, 192-236

Borcard, D., Legendre, P., & Drapeau, P. (1992). Partialling out the spatial component of ecological variation. *Ecology, 73*, 1045-1055

Carlson, K.M., Asner, G.P., Hughes, R.F., Ostertag, R., & Martin, R.E. (2007). Hyperspectral remote sensing of canopy biodiversity in Hawaiian lowland rainforests. *Ecosystems, 10*, 536-549

Clifford, P., Richardson, S., & Hemon, D. (1989). Assessing the significance of the correlation between two spatial processes. *Biometrics, 45*, 149-158

de Beurs, K.M., & Henebry, G.M. (2004). Land surface phenology, climatic variation, and institutional change: Analyzing agricultural land cover change in Kazakhstan. *Remote Sensing of Environment, 89*, 497-509

de Beurs, K.M., & Henebry, G.M. (2008a). Northern annular mode effects on the land surface phenologies of Northern Eurasia. *Journal of Climate, 21*, 4257-4279

de Beurs, K.M., & Henebry, G.M. (2008b). War, drought, and phenology: Changes in the land surface phenology of Afghanistan since 1982. *Journal of Land Use Science, 3*, 95-111

Fairbanks, D.H.K., & McGwire, K.C. (2004). Patterns of floristic richness in vegetation communities of California: Regional scale analysis with multi-temporal NDVI. *Global Ecology and Biogeography, 13*, 221-235

Ferrier, S. (2002). Mapping spatial pattern in biodiversity for regional conservation planning: Where to from here? *Systematic Biology, 51*, 331-363

Gitelson, A.A. (2004). Wide dynamic range vegetation index for remote quantification of biophysical characteristics of vegetation. *Journal of Plant Physiology, 161*, 165-173

Gitelson, A.A., Kaufman, Y.J., Stark, R., & Rundquist, D. (2002). Novel algorithms for remote estimation of vegetation fraction. *Remote Sensing of Environment, 80*, 76-87

Gitelson, A.A., Keydan, G.P., & Merzlyak, M.N. (2006a). Three-band model for noninvasive estimation of chlorophyll, carotenoids, and anthocyanin contents in higher plant leaves. *Geophysical Research Letters, 33*, L11402

Gitelson, A.A., Merzlyak, M.N., & Chivkunova, O.B. (2001). Optical properties and nondestructive estimation of anthocyanin content in plant leaves. *Photochemistry and Photobiology, 74*, 38-45

Gitelson, A.A., Viña, A., Masek, J.G., Verma, S.B., & Suyker, A.E. (2008). Synoptic monitoring of gross primary productivity of maize using Landsat data. *IEEE Geoscience and Remote Sensing Letters, 5*, 133-137

Gitelson, A.A., Viña, A., Verma, S.B., Rundquist, D.C., Arkebauer, T.J., Keydan, G., Leavitt, B., Ciganda, V., Burba, G.G., & Suyker, A.E. (2006b). Relationship between gross primary production and chlorophyll content in crops: Implications for the synoptic monitoring of vegetation productivity. *Journal of Geophysical Research-Atmospheres, 111*, D08S11

He, K.S., Zhang, J.T., & Zhang, Q.F. (2009). Linking variability in species composition and MODIS NDVI based on beta diversity measurements. *Acta Oecologica-International Journal of Ecology, 35*, 14-21

Henebry, G.M., Viña, A., & Gitelson, A.A. (2004). The wide dynamic range vegetation index and its potential utility for gap analysis. *GAP Analysis Program Bulletin, 12*, 50-56

Hofer, G., Wagner, H.H., Herzog, F., & Edwards, P.J. (2008). Effects of topographic variability on the scaling of plant species richness in gradient dominated landscapes. *Ecography, 31*, 131-139

Holben, B.N. (1986). Characteristics of maximum-value composite images from temporal AVHRR data. *International Journal of Remote Sensing, 7*, 1417-1434

Huete, A.R., Liu, H.Q., Batchily, K., & vanLeeuwen, W. (1997). A comparison of vegetation indices global set of TM images for EOS-MODIS. *Remote Sensing of Environment, 59*, 440-451

Jaccard, P. (1908). Nouvelles recherches sur la distribution florale. *Bull. Soc. Vaudoise Sci. Nat., 44*, 223-270

Jahan, N., & Gan, T.Y. (2009). Modeling gross primary production of deciduous forest using remotely sensed radiation and ecosystem variables. *Journal of Geophysical Research-Biogeosciences, 114*, G04026

Laurent, E.J., Shi, H.J., Gatziolis, D., LeBouton, J.P., Walters, M.B., & Liu, J. (2005). Using the spatial and spectral precision of satellite imagery to predict wildlife occurrence patterns. *Remote Sensing of Environment, 97*, 249-262

Lee, D.W., Brammeier, S., & Smith, A.P. (1987). The selective advantages of anthocyanins in developing leaves of mango and cacao. *Biotropica, 19*, 40-49

Legendre, P. (2000). Comparison of permutation methods for the partial correlation and partial Mantel tests. *Journal of Statistical Computation and Simulation, 67*, 37-73

Legendre, P., & Legendre, L. (1998). *Numerical Ecology*: Elsevier Science, The Netherlands

Lichstein, J.W., Simons, T.R., Shriner, S.A., & Franzreb, K.E. (2002). Spatial autocorrelation and autoregressive models in ecology. *Ecological Monographs, 72*, 445-463

Liu, J., & Ashton, P.S. (1999). Simulating effects of landscape context and timber harvest on tree species diversity. *Ecological Applications, 9*, 186-201

Loucks, C.J., Lu, Z., Dinerstein, E., Wang, D.J., Fu, D.L., & Wang, H. (2003). The giant pandas of the Qinling mountains, China: A case study in designing conservation landscapes for elevational migrants. *Conservation Biology, 17*, 558-565

McKnight, M.W., White, P.S., McDonald, R.I., Lamoreux, J.F., Sechrest, W., Ridgely, R.S., & Stuart, S.N. (2007). Putting beta-diversity on the map: Broad-scale congruence and coincidence in the extremes. *Plos Biology, 5*, 2424-2432

Morisette, J.T., Jarnevich, C.S., Ullah, A., Cai, W.J., Pedelty, J.A., Gentle, J.E., Stohlgren, T.J., & Schnase, J.L. (2006). A tamarisk habitat suitability map for the continental United States. *Frontiers in Ecology and the Environment, 4*, 11-17

Morisita, M. (1959). Measuring of the dispersion and analysis of distribution patterns. *Memoires of the Faculty of Science, Kyushu University, Series E. Biology., 2*, 215-235

Nagendra, H. (2001). Using remote sensing to assess biodiversity. *International Journal of Remote Sensing, 22*, 2377-2400

Nautiyal, M.C., Nautiyal, B.P., & Prakash, V. (2001). Phenology and growth from distribution in an alpine pasture at Tungnath, Garhwal, Himalaya. *Mountain Research and Development, 21*, 168-174

Negi, G.C.S., Rikhari, H.C., & Singh, S.P. (1992). Phenological features in relation to growth forms and biomass accumulation in an alpine meadow of the central Himalaya. *Vegetatio, 101*, 161-170

Pan, W., Gao, Z.S., & Lu, Z. (1988). *The giant panda's natural refuge in the Qinling mountains*. Beijing: Beijing University Press

Parker, A.J. (1982). The topographic relative moisture index: An approach to soil-moisture assessment in mountain terrain. *Physical Geography, 3*, 160-168

Perry, E.M., & Roberts, D.A. (2008). Sensitivity of narrow-band and broad-band indices for assessing nitrogen availability and water stress in an annual crop. *Agronomy Journal, 100*, 1211-1219

Rahbek, C. (1995). The elevational gradient of species richness - a uniform pattern. *Ecography, 18*, 200-205

Reid, D.G., & Hu, J. (1991). Giant panda selection between *Bashania fangiana* bamboo habitats in Wolong reserve, Sichuan, China. *Journal of Applied Ecology, 28*, 228-243

Roberts, D.A., Dennison, P.E., Peterson, S., Sweeney, S., & Rechel, J. (2006). Evaluation of airborne visible/infrared imaging spectrometer (AVIRIS) and moderate resolution imaging spectrometer (MODIS) measures of live fuel moisture and fuel condition in a shrubland ecosystem in Southern California. *Journal of Geophysical Research-Biogeosciences, 111*, G01S02.

Rocchini, D. (2007). Distance decay in spectral space in analysing ecosystem beta-diversity. *International Journal of Remote Sensing, 28*, 2635-2644

Rocchini, D., Balkenhol, N., Carter, G.A., Foody, G.M., Gillespie, T.W., He, K.S., Kark, S., Levin, N., Lucas, K., Luoto, M., Nagendra, H., Oldeland, J., Ricotta, C., Southworth, J., & Neteler, M. (2010). Remotely sensed spectral heterogeneity as a proxy of species diversity: Recent advances and open challenges. *Ecological Informatics, 5*, 318-329

Rouse, J.W., Haas, R.H., Schell, J.A., & Deering, D.W. (1973). Monitoring the vernal advancement and retrogradation (green wave effect) of natural vegetation. College Station, Remote Sensing Center, Texas A&M University.

Savitzky, A., & Golay, M.J.E. (1964). Smoothing and differentiation of data by simplified least squares procedures. *Analytical Chemistry, 36*, 1627-1639

Scott, J.M., Davis, F.W., McGhie, R.G., Wright, R.G., Groves, C., & Estes, J. (2001). Nature reserves: Do they capture the full range of America's biological diversity? *Ecological Applications, 11*, 999-1007

Stow, D., Niphadkar, M., & Kaiser, J. (2005). MODIS-derived visible atmospherically resistant index for monitoring chaparral moisture content. *International Journal of Remote Sensing, 26*, 3867-3873

Sun, W.X., Liang, S.L., Xu, G., Fang, H.L., & Dickinson, R. (2008). Mapping plant functional types from MODIS data using multisource evidential reasoning. *Remote Sensing of Environment, 112*, 1010-1024

Thessler, S., Ruokolainen, K., Tuomisto, H., & Tomppo, E. (2005). Mapping gradual landscape-scale floristic changes in Amazonian primary rain forests by combining ordination and remote sensing. *Global Ecology and Biogeography, 14*, 315-325

Tuanmu, M.-N., Viña, A., Bearer, S., Xu, W., Ouyang, Z., Zhang, H., & Liu, J. (2010). Mapping understory vegetation using phenological characteristics derived from remotely sensed data. *Remote Sensing of Environment, 114*, 1833-1844

Tuanmu, M.N., Viña, A., Roloff, G.J., Liu, W., Ouyang, Z.Y., Zhang, H.M., & Liu, J. (2011). Temporal transferability of wildlife habitat models: Implications for habitat monitoring. *Journal of Biogeography, 38*, 1510-1523

Tuomisto, H., Poulsen, A.D., Ruokolainen, K., Moran, R.C., Quintana, C., Celi, J., & Canas, G. (2003a). Linking floristic patterns with soil heterogeneity and satellite imagery in Ecuadorian Amazonia. *Ecological Applications, 13*, 352-371

Tuomisto, H., Ruokolainen, K., & Yli-Halla, M. (2003b). Dispersal, environment, and floristic variation of Western Amazonian forests. *Science, 299*, 241-244

Turner, W., Spector, S., Gardiner, N., Fladeland, M., Sterling, E., & Steininger, M. (2003). Remote sensing for biodiversity science and conservation. *Trends in Ecology & Evolution, 18*, 306-314

Vermote, E.F., ElSaleous, N., Justice, C.O., Kaufman, Y.J., Privette, J.L., Remer, L., Roger, J.C., & Tanre, D. (1997). Atmospheric correction of visible to middle-infrared EOS-MODIS data over land surfaces: Background, operational algorithm and validation. *Journal of Geophysical Research-Atmospheres, 102*, 17131-17141

Viña, A., Bearer, S., Zhang, H., Ouyang, Z., & Liu, J. (2008). Evaluating MODIS data for mapping wildlife habitat distribution. *Remote Sensing of Environment, 112*, 2160-2169

Viña, A., & Gitelson, A.A. (2005). New developments in the remote estimation of the fraction of absorbed photosynthetically active radiation in crops. *Geophysical Research Letters, 32*, L17403

Viña, A., & Gitelson, A.A. (2011). Sensitivity to foliar anthocyanin content of vegetation indices using green reflectance. *IEEE Geoscience and Remote Sensing Letters, 8*, 464-468

Viña, A., Gitelson, A.A., Rundquist, D.C., Keydan, G., Leavitt, B., & Schepers, J. (2004). Monitoring maize (Zea mays l.) phenology with remote sensing. *Agronomy Journal, 96*, 1139-1147

Viña, A., & Henebry, G.M. (2005). Spatio-temporal change analysis to identify anomalous variation in the vegetated land surface: ENSO effects in tropical South America. *Geophysical Research Letters, 32*, L21402

Viña, A., Tuanmu, M.-N., Xu, W., Li, Y., Ouyang, Z., DeFries, R., & Liu, J. (2010). Range-wide analysis of wildlife habitat: Implications for conservation. *Biological Conservation, 143*, 1960-1969

Vourlitis, G.L., Lobo, F.D., Zeilhofer, P., & Nogueira, J.D. (2011). Temporal patterns of net CO_2 exchange for a tropical semideciduous forest of the Southern Amazon basin. *Journal of Geophysical Research-Biogeosciences, 116*

Xiao, X.M., Hagen, S., Zhang, Q.Y., Keller, M., & Moore, B. (2006). Detecting leaf phenology of seasonally moist tropical forests in South America with multi-temporal MODIS images. *Remote Sensing of Environment, 103*, 465-473

Xiao, X.M., Zhang, Q.Y., Braswell, B., Urbanski, S., Boles, S., Wofsy, S., Berrien, M., & Ojima, D. (2004). Modeling gross primary production of temperate deciduous broadleaf forest using satellite images and climate data. *Remote Sensing of Environment, 91*, 256-270

Xiao, X.M., Zhang, Q.Y., Saleska, S., Hutyra, L., De Camargo, P., Wofsy, S., Frolking, S., Boles, S., Keller, M., & Moore, B. (2005). Satellite-based modeling of gross primary production in a seasonally moist tropical evergreen forest. *Remote Sensing of Environment, 94*, 105-122

Xu, W.H., Ouyang, Z., Viña, A., Zheng, H., Liu, J.G., & Xiao, Y. (2006). Designing a conservation plan for protecting the habitat for giant pandas in the Qionglai mountain range, China. *Diversity and Distributions, 12*, 610-619

Yue, M., Dang, G.D., & Yong, L.J. (1999). The basic features of vegetation of Foping nature reserve in Shaanxi province. *Journal of Wuhan Botanical Research, 17*, 22-28

Ziello, C., Estrella, N., Kostova, M., Koch, E., & Menzel, A. (2009). Influence of altitude on phenology of selected plant species in the alpine region (1971-2000). *Climate Research, 39*, 227-234

Table 1. Vegetation Indices evaluated in the study.

Index	Formulation	Reference
Normalized Difference Vegetation Index	$NDVI = \frac{\rho_{NIR} - \rho_{Red}}{\rho_{NIR} + \rho_{Red}}$	(Rouse et al. 1973)
Enhanced Vegetation Index	$EVI = 2.5 \frac{\rho_{NIR} - \rho_{Red}}{1 + \rho_{NIR} + 6\rho_{Red} - 7.5\rho_{Blue}}$	(Huete et al. 1997)
Wide-Dynamic Range Vegetation Index*	$WDRVI = \frac{\alpha \cdot \rho_{NIR} - \rho_{Red}}{\alpha \cdot \rho_{NIR} + \rho_{Red}}$	(Gitelson 2004)
Visible Atmospherically Resistant Index	$VARI = \frac{\rho_{Green} - \rho_{Red}}{\rho_{Green} + \rho_{Red} - \rho_{Blue}}$	(Gitelson et al. 2002)

*α = 0.2, as determined by a heuristic procedure (Henebry et al. 2004)

Table 2. Mantel correlation coefficients of the relationship between floristic similarity (using the Jaccard index for presence-absence data and the Morisita index for abundance data) and phenological similarity (using the Euclidean distance with a changed sign) calculated using four vegetation index image time series. Values in parentheses represent the correlation coefficients obtained from partial Mantel tests performed using a matrix of inter-plot geographic distances as a co-variable. All Mantel correlation coefficients were significant ($p < 0.001$) based on a Monte Carlo permutation test with 999 permutations.

	NDVI[1] (Euclidean)	WDRVI[2] (Euclidean)	EVI[3] (Euclidean)	VARI[4] (Euclidean)
Tree species (Jaccard)	0.152 (0.148)	0.203 (0.208)	0.280 (0.288)	0.255 (0.258)
Tree species (Morisita)	0.140 (0.135)	0.177 (0.181)	0.213 (0.220)	0.235 (0.238)
Tree & bamboo species (Jaccard)	0.191 (0.187)	0.242 (0.249)	0.307 (0.317)	0.325 (0.331)

[1]Normalized Difference Vegetation Index; [2]Wide Dynamic Range Vegetation Index; [3]Enhanced Vegetation Index; [4]Visible Atmospherically Resistant Index

Table 3. Coefficients of the multiple linear regression models between the Non-Metric Multidimensional Scaling (NMDS) axes (dependent variables) obtained from the floristic similarity (Jaccard index for presence-absence of tree and bamboo species) among 104 field plots, and the first six principal components (PC) obtained from 46 eight-day maximum value composite image time series of the Visible Atmospherically Resistant Index (VARI). Values in parentheses represent standard errors of model coefficients.

Variable	NMDS Axis 1	NMDS Axis 2
	OLS (SE)	SAR (SE)
Intercept	-0.0004 (0.0033)	-0.0004 (0.0035)
PC1	0.1943[§] (0.0126)	-0.0194 (0.0132)
PC2	0.0454 (0.0250)	-0.1403[§] (0.0292)
PC3	-0.1692[†] (0.0693)	-0.0710 (0.0727)
PC4	0.7582[§] (0.0859)	0.2142[*] (0.0922)
PC5	0.0105 (0.1708)	-0.2890 (0.1792)
PC6	0.9241[†] (0.2979)	-0.2662 (0.3188)
Spatial lag	N/A	0.4211[§] (0.0970)
R^2	0.7821	0.5235

OLS – Ordinary least squares model; SAR – Spatial auto-regressive model; SE – Standard error; [*]$p < 0.05$; [†]$p < 0.01$; [§]$p<0.001$.

Figure Legends

Fig. 1. Topographic map of the study region (i.e., Qinling Mountains) showing the location and extent of nature reserves and of the 104 circular field plots (black dots) established during the summers of 2007 and 2008.

Fig. 2. Temporal profiles of the (A) average, (B) standard deviation and (C) Pearson's correlation coefficient with elevation, of the four different vegetation indices evaluated (see Table 1), obtained from the pixels where the field plots were located.

Fig. 3. Average structural characteristics (A: canopy closure; B: basal area; C: stem density; D: tree species richness) of the forests studied among different elevation ranges. Elevation ranges with different letters exhibit significantly ($p < 0.01$) different structural characteristics, as determined by Bonferroni-corrected post-hoc Mann-Whitney U tests. Error bars correspond to 2 SEM.

Fig. 4. Two-dimensional ordination space derived from a non-metric multidimensional scaling (NMDS) procedure applied to the floristic similarity among 104 field plots, using the Jaccard index for presence-absence of tree and bamboo species. Symbol letters in (A) correspond to different elevation ranges (i.e., a: 1000-1500m; b: 1500-2000m; c: 2000-2500m; d: 2500-3000m). Symbol numbers in (B) correspond to aspect [converted into soil moisture classes (Parker 1982), ranging from dry=1 to wet=20]. Symbol letters in (C) correspond to different slope ranges (i.e., A: <10°; B: 11-20°; C: 21-30°; D: >30°).

Symbol letters in (D) correspond to different forest types (i.e., D: predominantly deciduous broadleaf; M: mixed coniferous-deciduous; C: predominantly coniferous).

Fig. 5. Linear regressions of (A) axis 1 of the Non-Metric Multidimensional Scaling (NMDS) procedure applied to the floristic similarity among 104 field plots, using the Jaccard index for presence-absence of tree and bamboo species, and (B) first component of the principal component analysis (PCA) applied to 46 eight-day maximum value composite image time series of the Visible Atmospherically Resistant Index (VARI), vs. elevation. Regression lines are significant ($p < 0.05$) after accounting for spatial autocorrelation (Clifford et al. 1989).

Fig. 6. Principal component (PC) loadings (which indicate the correlation of each component with members of the original image time series) of the first six principal components obtained from the eight-day maximum value composite image time series (46 images) of the Visible Atmospherically Resistant Index (VARI).

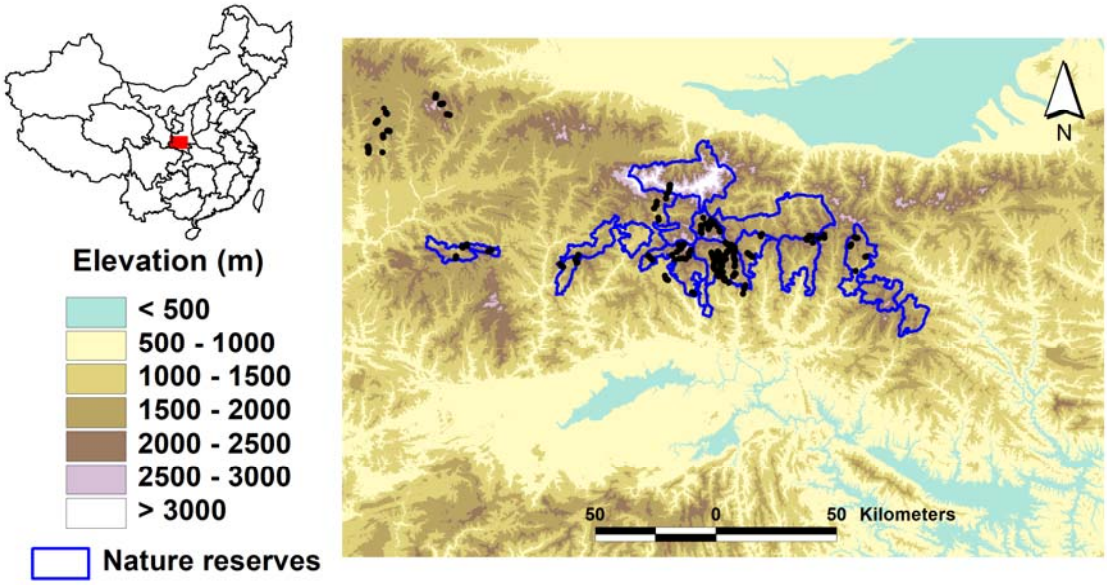
Elevation (m)
< 500
500 - 1000
1000 - 1500
1500 - 2000
2000 - 2500
2500 - 3000
> 3000
Nature reserves
N
50
0
50 Kilometers

Fig. 1

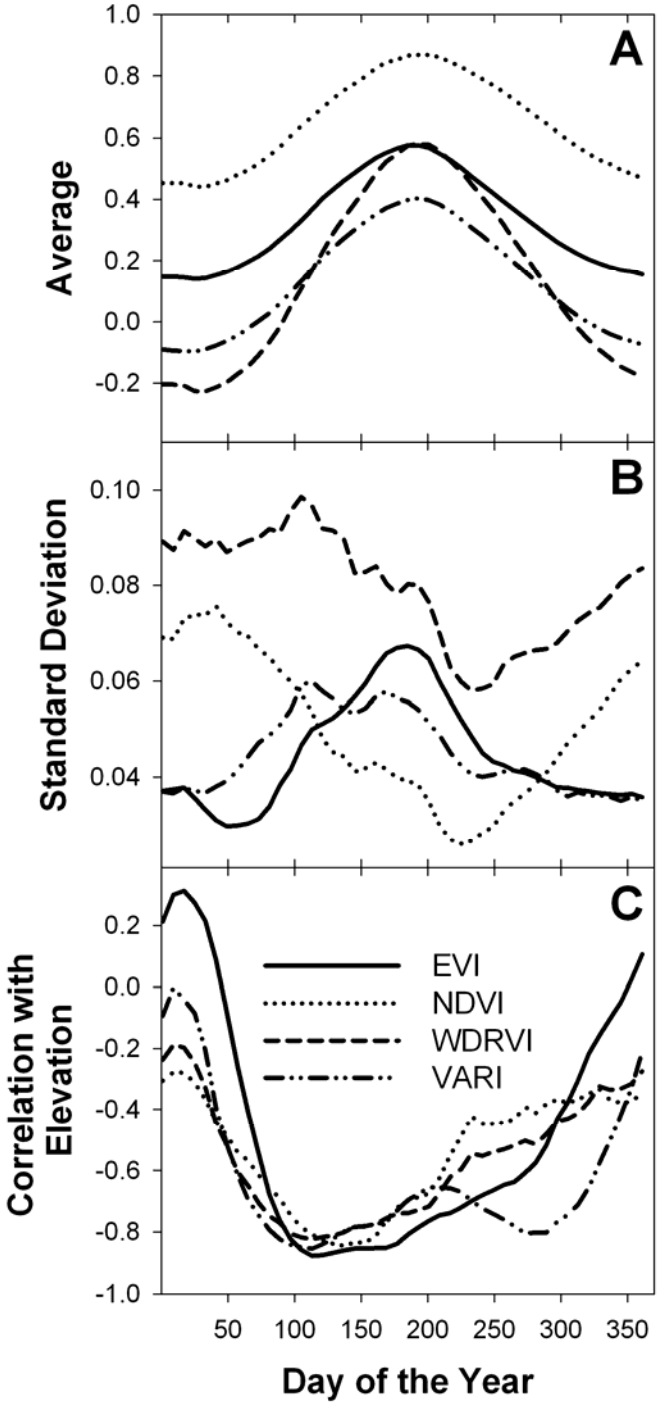
A
B
C
Average
Standard Deviation
Correlation with Elevation
EVI
NDVI
WDRVI
VARI
Day of the Year
1.0
0.8
0.6
0.4
0.2
0.0
-0.2
0.10
0.08
0.06
0.04
0.2
0.0
-0.2
-0.4
-0.6
-0.8
-1.0
50
100
150
200
250
300
350

Fig 2.

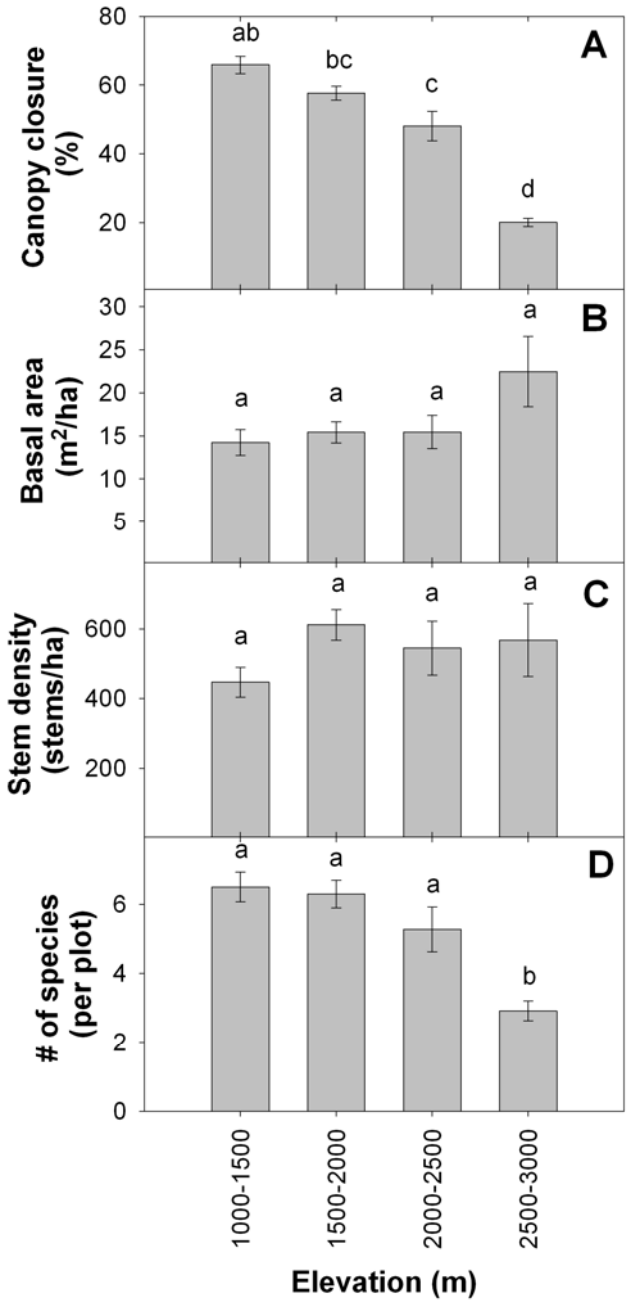
A
B
C
D
Canopy closure (%)
Basal area (m2/ha)
Stem density (stems/ha)
# of species (per plot)
ab
bc
c
d
a
a
a
a
a
a
a
a
a
a
a
b
1000-1500
1500-2000
2000-2500
2500-3000
Elevation (m)

Fig. 3

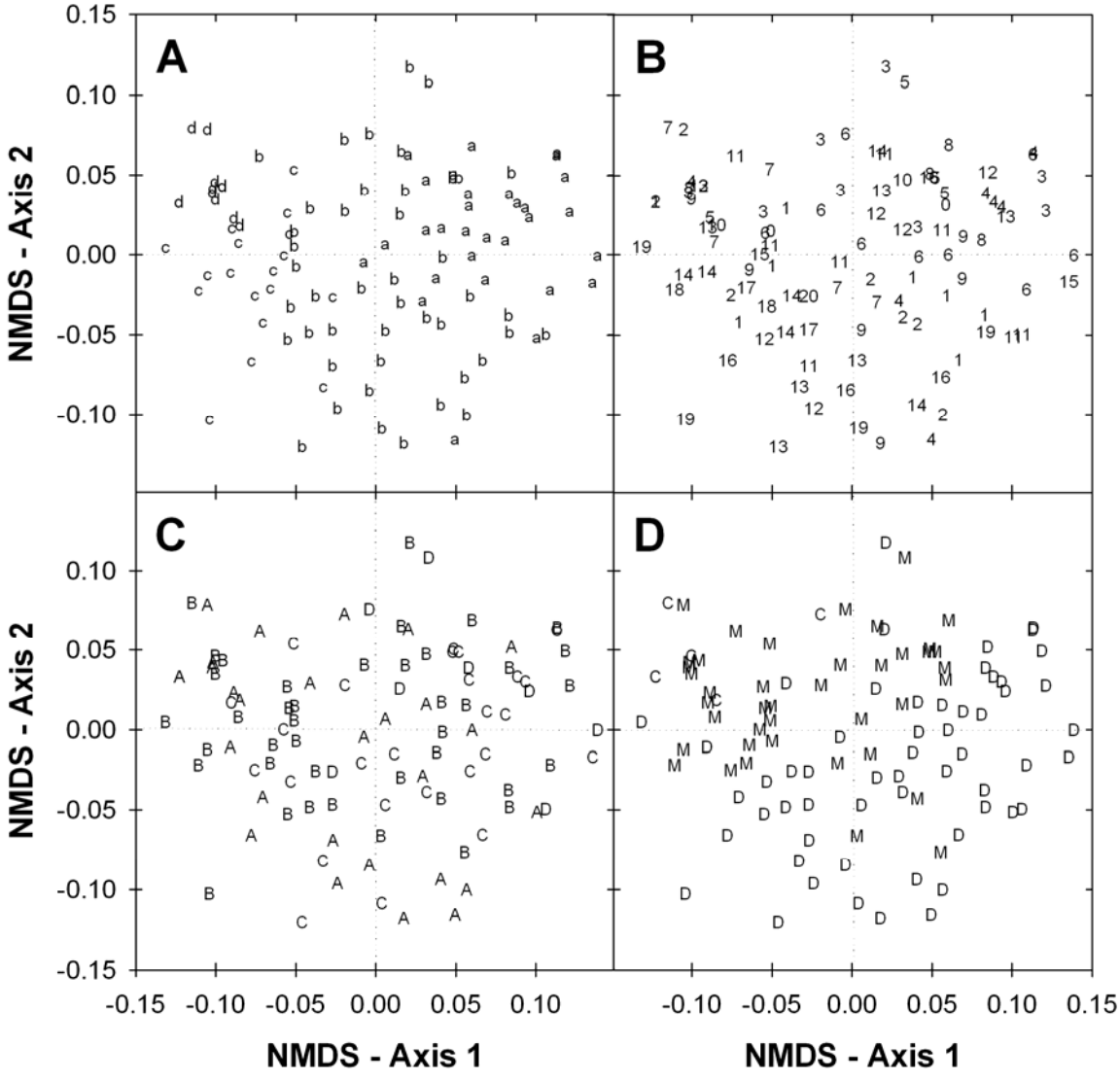

Fig. 4

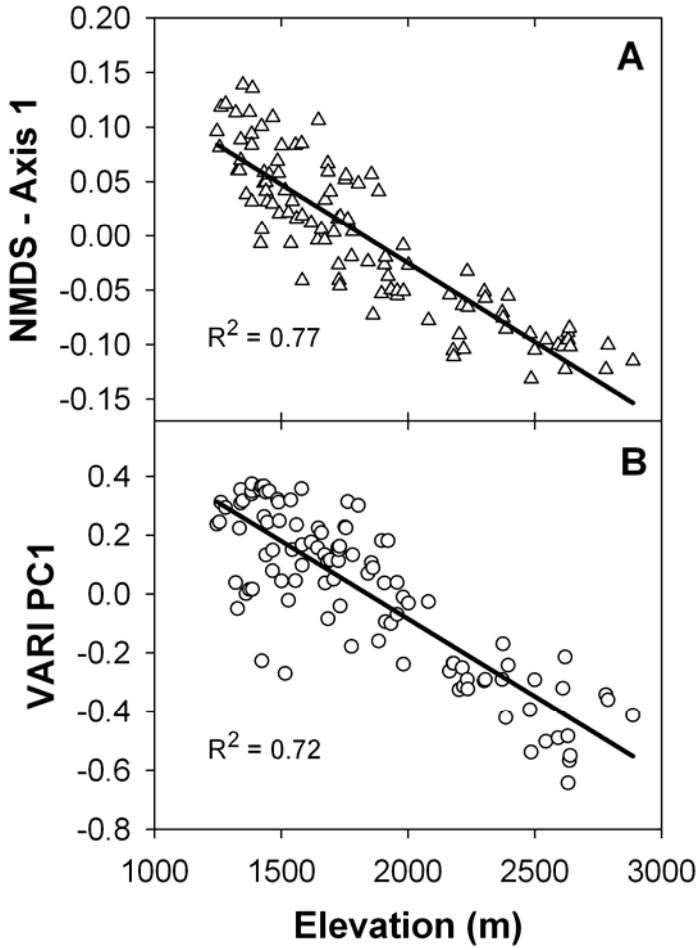
A
B
NMDS - Axis 1
VARI PC1
R^2 = 0.77
R^2 = 0.72
0.20
0.15
0.10
0.05
0.00
-0.05
-0.10
-0.15
0.4
0.2
0.0
-0.2
-0.4
-0.6
-0.8
1000
1500
2000
2500
3000
Elevation (m)

Fig. 5

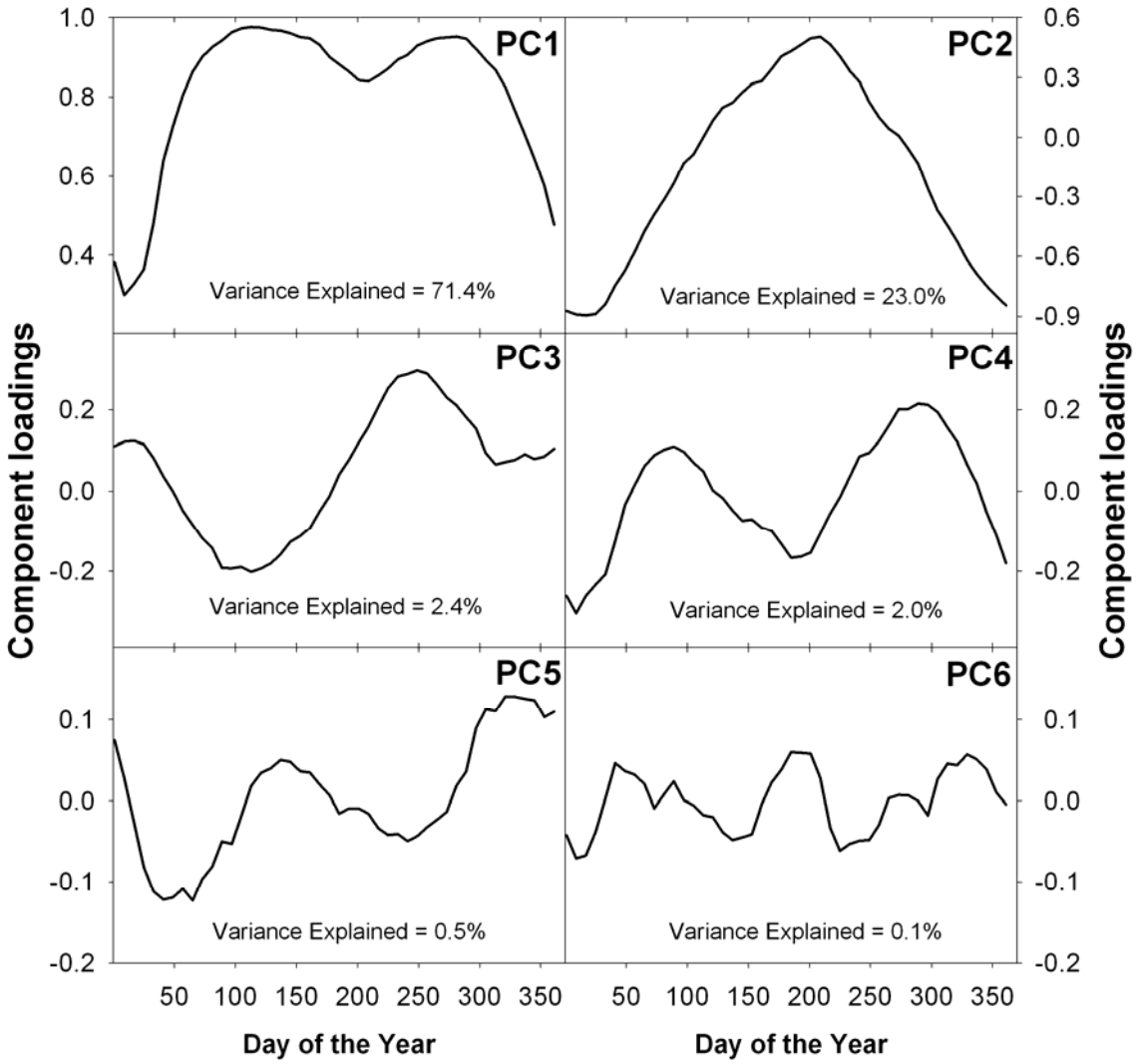
PC1
Variance Explained = 71.4%
PC2
Variance Explained = 23.0%
PC3
Variance Explained = 2.4%
PC4
Variance Explained = 2.0%
PC5
Variance Explained = 0.5%
PC6
Variance Explained = 0.1%
Component loadings
Component loadings
Day of the Year
Day of the Year

Fig. 6

On-line Supplementary Data for:

Relationship between floristic similarity and vegetated land surface phenology: Implications for the synoptic monitoring of species diversity at broad geographic regions

Andrés Viña[1], Mao-Ning Tuanmu[1], Weihua Xu[2], Yu Li[1], Jiaguo Qi[3], Zhiyun Ouyang[2] and Jianguo Liu[1]

[1] Center for Systems Integration and Sustainability, Department of Fisheries and Wildlife, Michigan State University, East Lansing, MI, USA; [2] State Key Lab of Urban and Regional Ecology, Research Center for Eco-Environmental Sciences, Chinese Academy of Sciences, Beijing, China; [3] Center for Global Change and Earth Observations, Department of Geography, Michigan State University, East Lansing, MI, USA

Corresponding Author: Andrés Viña
Center for Systems Integration and Sustainability
1405 S. Harrison Road
Suite 115 Manly Miles Bldg.
Michigan State University
East Lansing, MI 48823-5243
U. S. A.
Phone: (517) 432-5078
e-mail: vina@msu.edu

Published in Remote Sensing of Environment 121 (2012), pages: 488–496

List of families and species of trees found in 104 field plots established in temperate montane forests of the Qinling Mountains region, Shaanxi province, China.

ACERACEAE
- *Acer cappadocicum* Rehd.
- *Acer davidii* Franchet
- *Acer franchetii* Pax
- *Acer ginnala* Maxim.
- *Acer henryi* Pax.
- *Acer maximowiczii* Pax
- *Acer pictum* subsp. *mono* (Maximowicz) H. Ohashi
- *Acer shensiense* Fang
- *Acer truncatum* Bunge
- *Dipteronia sinensis* Oliver

ADOXACEAE
- *Viburnum betulifolium* Batalin
- *Viburnum dilatatum* Thunb.

ALANGIACEAE
- *Alangium chinense* (Loureiro) Harms

ANACARDIACEAE
- *Cotinus coggygria* Scopoli
- *Rhus punjabensis* var. *sinica* (Diels) Rehder & E. H. Wilson
- *Toxicodendron vernicifluum* (Stokes) F. A. Barkley

AQUIFOLIACEAE
- *Ilex pernyi* Franchet

ARALIACEAE
- *Kalopanax septemlobus* (Thunberg) Koidzumi

BETULACEAE
- *Betula albo-sinensis* Burkill
- *Betula albo-sinensis* var. *septentrionalis* Schneider
- *Betula luminifera* H. Winkler
- *Betula platyphylla* Sukaczev
- *Carpinus cordata* Blume
- *Carpinus polyneura* Franchet
- *Carpinus turczaninowii* Hance
- *Corylus chinensis* Franchet
- *Corylus ferox* var. *thibetica* (Batalin) Franchet
- *Corylus heterophylla* Fischer ex Trautvetter
- *Corylus mandshurica* Maximowicz

CAPRIFOLIACEAE
- *Lonicera hispida* Pall. ex Roem. et Schult.

CELASTRACEAE
- *Euonymus alatus* (Thunberg) Siebold
- *Euonymus phellomanus* Loesener

CERCIDIPHYLLACEAE
Cercidiphyllum japonicum Siebold & Zuccarini
CORNACEAE
Cornus controversa Hemsley
Cornus hemsleyi C. K. Schneider & Wangerin
Cornus macrophylla Wallich
Cornus sp.
Dendrobenthamia japonica var. chinensis (Osborn) Fang
CUPRESSACEAE
Juniperus chinensis Linnaeus
ERICACEAE
Rhododendron purdomii Rehder & E. H. Wilson
EUPTELEACEAE
Euptelea pleiosperma J. D. Hooker & Thomson
FABACEAE
Cercis chinensis Bunge
Maackia hupehensis Takeda
Ormosia henryi Prain
FAGACEAE
Castanea sp.
Cyclobalanopsis oxyodon (Miquel) Oersted
Quercus aliena Blume
Quercus aliena var. *acutiserrata* Maximowicz ex Wenzig
Quercus glandulifera Blume
Quercus spinosa David ex Franchet
Quercus variabilis Blume
Quercus wutaishanica Mayr
FLACOURTIACEAE
Idesia polycarpa Maximowicz
HAMAMELIDACEAE
Fortunearia sinensis Rehder & E. H. Wilson
Sinowilsonia henryi Hemsley
JUGLANDACEAE
Juglans cathayensis Dode
Platycarya strobilacea Siebold & Zuccarini
Pterocarya stenoptera C. de Candolle
LAURACEAE
Lindera glauca (Siebold & Zuccarini) Blume
Lindera obtusiloba Blume
Litsea pungens Hemsley
Sassafras tzumu (Hemsley) Hemsley
MAGNOLIACEAE
Magnolia biondii Pamp.
MELIACEAE
Toona sinensis (A. Jussieu) M. Roemer

MORACEAE
Morus alba Linnaeus
OLEACEAE
Fraxinus chinensis Roxburgh
Fraxinus mandschurica Ruprecht
Ligustrum lucidum W. T. Aiton
PINACEAE
Abies chensiensis Tieghem
Abies fargesii Franchet
Larix chinensis Beissn.
Larix principis-rupprechtii Mayr
Picea wilsonii Mast.
Pinus armandii Franchet
Pinus tabuliformis Carrière
Tsuga chinensis (Franchet) E. Pritzel
RHAMNACEAE
Rhamnus utilis Decaisne
ROSACEAE
Crataegus kansuensis E. H. Wilson
Crataegus pinnatifida var. *major* N. E. Brown
Maddenia hypoxantha Koehne
Malus hupehensis (Pampanini) Rehder
Prunus scopulorum Koehne
Prunus sp.
Pyrus betulifolia Bunge
Pyrus xerophila T. T. Yu
Sorbus alnifolia (Siebold & Zuccarini) K. Koch
Sorbus koehneana C. K. Schneider
Sorbus sp.
SABIACEAE
Meliosma cuneifolia Franchet
Meliosma oldhamii Miquel ex Maximowicz
SALICACEAE
Populus davidiana Dode
Populus purdomii Rehder
Populus szechuanica C. K. Schneider
Populus wilsonii C. K. Schneider
Salix matsudana Koidz.
Salix pseudotangii C. Wang & C. Y. Yu
Salix sp.
Salix variegata Franchet
SAPINDACEAE
Aesculus chinensis Bunge
Koelreuteria paniculata Laxmann
SAXIFRAGACEAE
Deutzia scabra Thunb.

SIMAROUBACEAE
Ailanthus altissima (Miller) Swingle
STAPHYLEACEAE
Staphylea holocarpa Hemsley
SYMPLOCACEAE
Symplocos paniculata (Thunberg) Miquel
THEACEAE
Stewartia shensiensis Hung T. Chang
TILIACEAE
Tilia chinensis Maximowicz
Tilia mandshurica Ruprecht & Maximowicz
Tilia paucicostata Maximowicz
ULMACEAE
Celtis koraiensis Nakai
Celtis sinensis Persoon
Ulmus bergmanniana C. K. Schneider
Ulmus macrocarpa Hance
Ulmus parvifolia Jacquin
Ulmus pumila Linnaeus
VERBENACEAE
Clerodendrum trichotomum Thunberg